Received: 10 July 2019 | Revised: 13 September 2019 | Accepted: 13 September 2019

DOI: 10.1002/mrm.28029

FULL PAPER

Magnetic Resonance in Medicine

Rapid and motion-robust volume coverage using cross-sectional real-time MRI

Dirk Voit | **Oleksandr Kalentev** | **Maaike van Zalk** | **Arun A. Joseph** | **Jens Frahm**

Biomedizinische NMR, Max-Planck-Institut für biophysikalische Chemie, Göttingen, Germany

Correspondence
Jens Frahm, Max-Planck-Institut für biophysikalische Chemie, Am Fassberg 11, 37070 Göttingen, Germany.
Email: jfrahm@gwdg.de

Purpose: To develop a rapid and motion-robust technique for volumetric MRI, which is based on cross-sectional real-time MRI acquisitions with automatic advancement of the slice position.

Methods: Real-time MRI with a frame-by-frame moving cross-section is performed with use of highly undersampled radial gradient-echo sequences offering spin density, T_1, or T_2/T_1 contrast. Joint reconstructions of serial images and coil sensitivity maps from spatially overlapping sections are accomplished by nonlinear inversion with regularization to the preceding section—formally identical to dynamic real-time MRI. Shifting each frame by 20% to 25% of the section thickness ensures 75% to 80% overlap of successive sections. Acquisition times of 40 to 67 ms allow for rates of 15 to 25 sections per second, while volumes are defined by the number of cross-sections times the section shift.

Results: Preliminary realizations at 3T comprise studies of the human brain, carotid arteries, liver, and prostate. Typically, coverage of a 90- to 180-mm volume at 0.8- to 1.2-mm in-plane resolution, 4- to 6-mm section thickness, and 0.8- to 1.5-mm section shift is accomplished within total measuring times of 4 to 6 seconds and a section speed of 15 to 37.5 mm per second. However, spatiotemporal resolution, contrast including options such as fat saturation and total measuring time are highly variable and may be adjusted to clinical needs. Promising volumetric applications range from fetal MRI to dynamic contrast-enhanced MRI.

Conclusion: The proposed method allows for rapid and motion-robust volume coverage in a variety of imaging scenarios.

KEYWORDS

nonlinear inverse reconstruction, real-time MRI, volume coverage

1 | INTRODUCTION

Efficient volume coverage at high spatiotemporal resolution and with different contrasts is a desirable option in many clinical imaging scenarios. Specific aims range from rapid localization issues in arbitrary body parts to studies of uncooperative patients or repetitive scans monitoring dynamic contrast enhancement (DCE). Because conventional multislice MRI is often too slow or even suffers from incomplete coverage, practical solutions commonly arise from

accelerated 3D MRI techniques with volumetric excitation and 3D encoding. However, such methods bear the inherent disadvantages of motion sensitivity and postacquisition reconstruction given that all data are required for a 3D image, that is, the relevant temporal "footprint" equals the total acquisition time.

In contrast, this work proposes to exploit recent advances toward cross-sectional real-time MRI[1,2] to achieve rapid and motion-robust scanning of a volume by an automatic positional advancement of each frame. Provided that successive frames (i.e., sections) exhibit sufficient spatial overlap, the concept simply takes advantage of the similarity of successive images: now in space rather than in time as for dynamic real-time MRI. In fact, such applications may be realized with the same reconstruction algorithm by regularized nonlinear inversion (NLINV), which allows for high-quality serial images at rates of 20 to 50 frames per second.[1] The proposed method bears some resemblance to continuously moving table MRI in combination with parallel imaging; for example, see previous works.[3-6] Although preliminary moving-table results have also been obtained by adopting NLINV,[7] such methods seem to be best suited for scanning very large volumes or even the whole body, whereas a routine diagnostic workup benefits from a more standardized (fixed) position of the patient. Moreover, in contrast to continuously moving table techniques, reconstructions of the proposed method do not suffer from k-space inconsistencies given that the position of the section only advances framewise.

It is important to recognize that the proposed volume coverage is not a 3D MRI technique because it lacks volumetric excitation and spatial encoding in all 3 dimensions. In fact, data acquisition as well as image reconstruction and display of individual cross-sections are in real time, while the position of the section moves each frame to scan a predefined volume. This concept of rapid cross-sectional volume coverage by real-time gradient-echo MRI bears several advantages: It is relatively fast, offers different contrasts, has minimized sensitivity to susceptibility artifacts, and with acquisition times of tens of milliseconds individual sections are robust against patient or organ movements. The approach may be particularly useful in several areas such as, for example, volumetric studies of breathing-affected or otherwise moving organs, studies of less cooperative patients or children with possible extensions to fetal imaging, applications to rapid time-of-flight angiography, and dynamic volumetric scanning before, during, and after contrast agent such as in DCE studies of the liver and prostate.

2 | METHODS

All MRI measurements were performed at 3T (Magnetom Prisma fit; Siemens Healthineers, Erlangen, Germany) with use of the standard 64-channel head coil or an 18-element thorax coil in conjunction with suitable elements of the spine coil array. During technical development, 12 subjects without known illness were recruited among the students of the local university. Written informed consent, according to the recommendations of the local ethics committee, was obtained from all subjects before MRI.

Rapid cross-sectional scanning of a volume is accomplished by highly undersampled radial gradient-echo sequences. Serial real-time acquisitions automatically advance the position of each cross-section by around 20% to 25% of the section thickness (i.e., 75–80% overlap) to ensure sufficient spatial similarity. On the user interface, the volume to be scanned is predefined by the number of cross-sections times the chosen section shift. For example, 100 cross-sections with 1.5-mm positional shift result in a 150-mm volume. Moreover, the sign of the section shift determines the starting point and direction of the measurement (i.e., the cross-sectional progress). For example, brain volumes in a transverse orientation may be obtained in the head-feet or feet-head direction and accordingly result in different presaturation effects on flowing spins. Typically, the sequential cross-sectional acquisitions use 5 successive sections with sets of complementary radial spokes as previously developed for serial imaging with radial trajectories.[1,8]

Table 1 summarizes a list of protocols and acquisition parameters tested here. Because the underlying MRI technique represents a generic gradient-echo sequence, the proposed method offers access to spin density and T_1 contrast for randomized radiofrequency spoiling[9] as well as to T_2/T_1-type contrasts for refocused fast low angle shot (FLASH) or reverse and fully balanced steady-state free precession (SSFP) conditions as controlled by respective gradient switching schemes. Further variants add preceding fat suppression[10,11] and/or spatial presaturation modules.[12] The broad range of imaging scenarios which are expected to benefit from the proposed method are studied by exemplary applications to the brain, carotid arteries, liver, and prostate.

Similar to dynamic real-time MRI, serial image reconstruction represents a nonlinear inverse problem. This is because the movement of a cross-section through a larger volume causes a continuous change of receive coil contributions and respective sensitivity maps. Accordingly, both the desired image and the actual sensitivity maps have to be jointly determined from the few data acquired for the actual frame—a task readily accomplished by NLINV as described in detail in a previous work.[1] In fact, without changes to the algorithm, the *spatial* fidelity of the current NLINV reconstruction matches its *temporal* fidelity as previously assessed using a dedicated motion phantom.[13] This performance is ensured and best understood by the fact that the iterative Gauss–Newton algorithm chosen to solve the nonlinear inverse problem[14] downsizes all regularization terms (relative

TABLE 1 Protocols and acquisition parameters for rapid volume coverage

	Brain	Brain	Carotids	Liver	Prostate
Contrast	T_1	T_2/T_1	Angio	T_1 + FS	T_2/T_1 + FS
Volume/mm	150	150	128	180	90
Field of view/mm^2	224 × 224	224 × 224	192 × 192	384 × 384	256 × 256
Image matrix	224 × 224	224 × 224	240 × 240	320 × 320	256 × 256
Resolution/mm^2	1.0 × 1.0	1.0 × 1.0	0.8 × 0.8	1.2 × 1.2	1.0 × 1.0
Thickness/mm	6	6	4	6	4
Section shift/mm	1.5 (25%)	1.5 (25%)	0.8 (20%)	1.5 (25%)	1.0 (25%)
TR/TE/ms	2.67/1.76	3.64/1.82	3.08/1.85	2.40/1.60	3.66/1.82
Spokes per section	15	13	13	19	17
Flip angle/degree	20	30	30	16	30
Time per section/ms	40.0	50.0	40.0	50.0[a]	66.7[a]
Number of sections	100	100	160	120	90
Time per volume/sec	4.0	5.0	6.4	6.0	6.0
Undersampling factor[b]	23.4	27	29	26.4	23.6

[a]Including repetitive fat saturation (FS = 13.4 ms) after every 3 frames.
[b]With reference to a fully sampled radial acquisition ($\pi/2$ × matrix resolution).

to the data consistency term) by a factor of 2 in each iterative step. In this study, applications to the brain and prostate use 7 iterations, whereas applications to the liver use 6 Newton steps. Postprocessing involves a temporal median filter matching the 5 frames with complementary spokes,[1] whereas image denoising takes advantage of a modified nonlocal means filter.[15]

Online reconstruction and display of cross-sectional images is achieved by a highly parallelized version of the NLINV algorithm and its implementation on a computer (Sysgen, Bremen, Germany), which was equipped with 8 graphical processing units (GPUs; GeForce GTX, TITAN; NVIDIA, Santa Clara, CA) and fully integrated into the reconstruction pipeline of the commercial MRI system.

3 | RESULTS

To assess the range of usable section shifts, or conversely to determine the required spatial overlap of successive sections, Figure 1 compares T_2/T_1-weighted brain images obtained with a section shift of 10%, 25%, and 50% of section thickness (here corresponding to 0.6, 1.5, and 3.0 mm, respectively) to a reference image with fully sampled radial trajectory (351 instead of 13 spokes) and fast Fourier transform (FFT) reconstruction. Although a 10% section shift ensures the best similarity of successive sections for serial NLINV reconstruction with regularization to the preceding section, the resulting images (Figure 1, top left) exhibit a certain degree of blurring when compared to a fully sampled image at 27 times the measuring time (Figure 1, bottom right). A 25% section shift (Figure 1, top right) may still be used when emphasizing speed (as chosen here for methodological description), whereas a section shift of 50% (Figure 1, bottom left) turns out to be too large given that it markedly increases blurring and, for the case of a T_2/T_1-weighted acquisition, further compromises contrast. This is because contributing magnetizations no longer experience enough excitations to establish a proper steady state of transverse coherences.

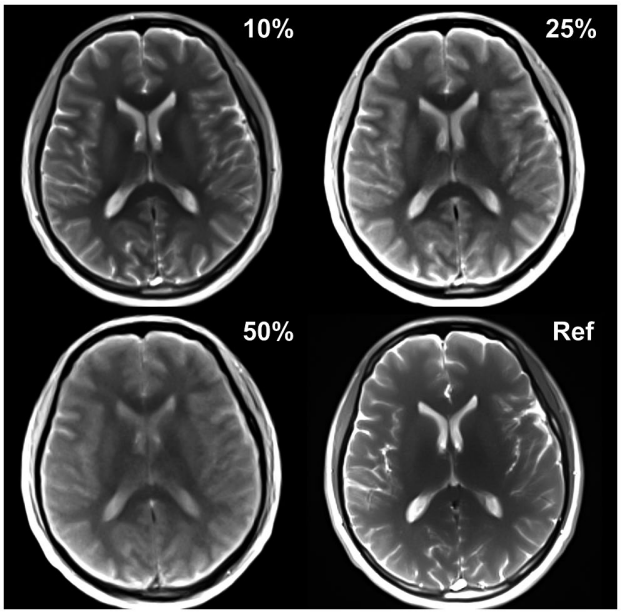

FIGURE 1 T_2/T_1-weighted brain images (13 spokes, 1.0 × 1.0 × 6.0 mm^3 nominal resolution) obtained with rapid volume coverage and section shifts of 10% (0.6 mm), 25% (1.5 mm), and 50% (3.0 mm), respectively, in comparison to a reference image with full radial sampling (351 spokes) and FFT reconstruction

Figure 2 depicts equidistant sections of a 5.0-second volumetric brain scan of a healthy volunteer (150-mm volume = 100 sections with a 25% or 1.5-mm section shift) at 1.0-mm nominal resolution; for the full movie, see Supporting Information Video S1. The T_2/T_1 contrast was obtained with use of a refocused FLASH acquisition (i.e., rephased radial encoding gradients in each repetition interval) with tune-up shim conditions (i.e., baseline homogeneity of the magnet without additional shimming). The latter could be realized because—in contrast to fully balanced SSFP MRI—the sequence does not suffer from banding artifacts. Of course, both reverse and fully balanced SSFP acquisitions are also possible (but require shimming) as are T_1-weighted spoiled FLASH measurements. A 4.0-second T_1-weighted brain scan covering the same volume as for Supporting Information Video S1 is shown in Supporting Information Video S2. While the chosen spatiotemporal resolution of these examples emphasizes speed as, for example, required for less cooperative patients or children, the total measuring time may be easily traded for larger volumes (i.e., more sections), thinner sections or smaller section shifts (i.e., more sections per volume), or higher in-plane resolution (i.e., longer acquisition times per section).

A strongly T_1-weighted 6.4-second volumetric scan of the neck region (128 mm volume = 160 sections with 0.8-mm section shift) at 0.8-mm in-plane resolution is depicted in Figure 3. The corresponding transverse sections (40 ms) are characterized by a pronounced and steady in-flow effect in Supporting Information Video S3. The resulting signal enhancement may be exploited for angiographic purposes, that is, a quick visualization of the carotid arteries by means of a maximum intensity projection of all acquired sections (Figure 3, right). To emphasize arterial flow at the expense of venous return, the neck volume was acquired top-down in the head-to-feet direction. A limitation of the angiographic application is given for studies of highly pulsatile flow, which in diastolic low-flow phases leads to sections with increased saturation. In maximum intensity projections, the effect appears as a dark band perpendicular to the affected vessel. While barely recognizable in the common carotid artery (Figure 3, right), more prominent appearances in the inferior vena cava and descending aorta (not shown) may impair a diagnostic assessment.

The motion robustness of volume coverage by cross-sectional real-time MRI is demonstrated in Figure 4 for a 6.0-second liver scan (180-mm volume = 120 sections with 1.5-mm section shift) obtained at 50-ms resolution during free breathing; see Supporting Information Video S4.

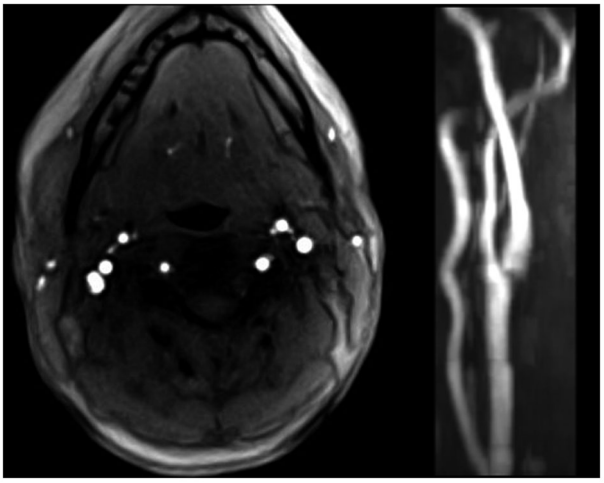

FIGURE 3 Selected T_1-weighted image of a 6.4-second real-time MRI acquisition (128-mm volume) and corresponding maximum intensity projection covering the carotid arteries (single side) of a healthy subject at 40.0 ms and $0.8 \times 0.8 \times 4.0$ mm^3 resolution. For details, see Table 1

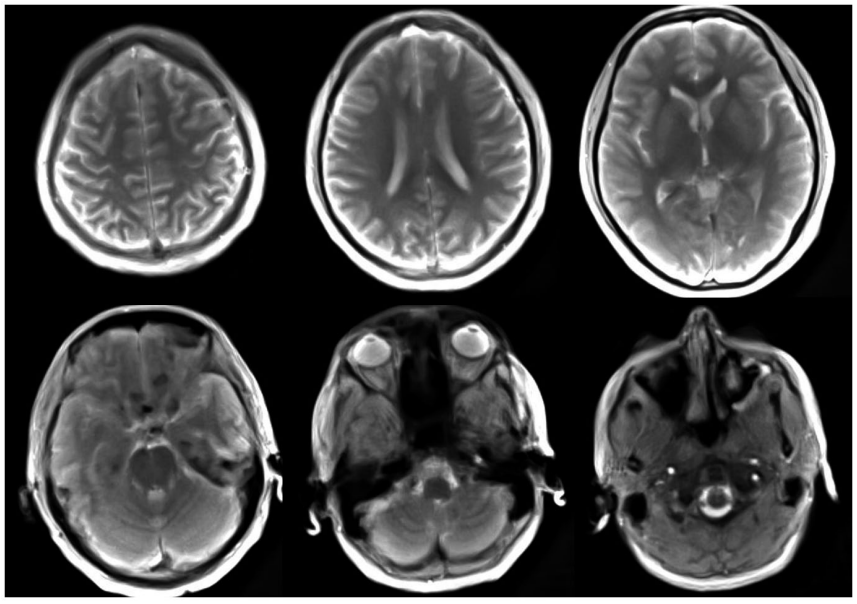

FIGURE 2 Selected T_2/T_1-weighted images (every 15th) of a 5.0-second real-time MRI acquisition covering the brain (150-mm volume) of a healthy subject at 50.0 ms and $1.0 \times 1.0 \times 6.0$ mm^3 resolution. For details, see Table 1

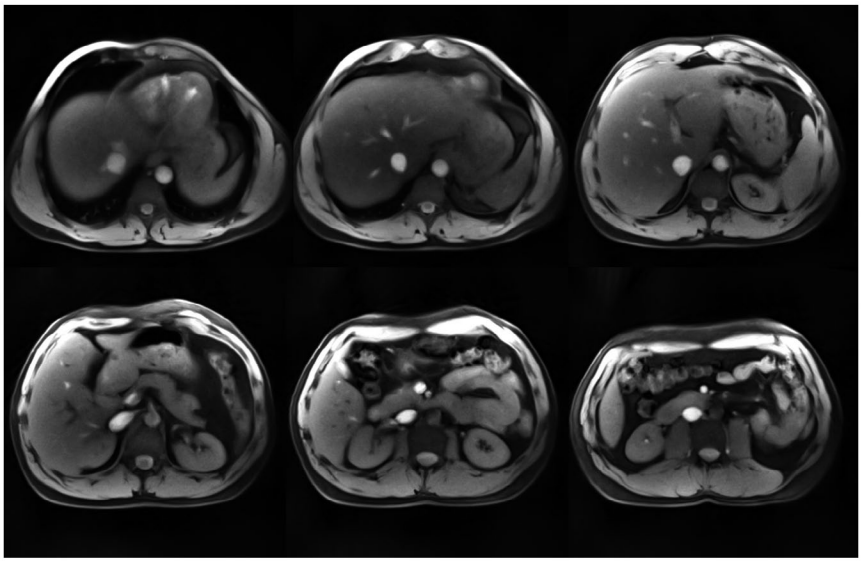

FIGURE 4 Selected fat-suppressed T_1-weighted images (every 20th) of a 6.0-second real-time MRI acquisition covering the liver (180-mm volume) of a healthy subject at 50.0 ms and $1.2 \times 1.2 \times 6.0$ mm^3 resolution. For details, see Table 1

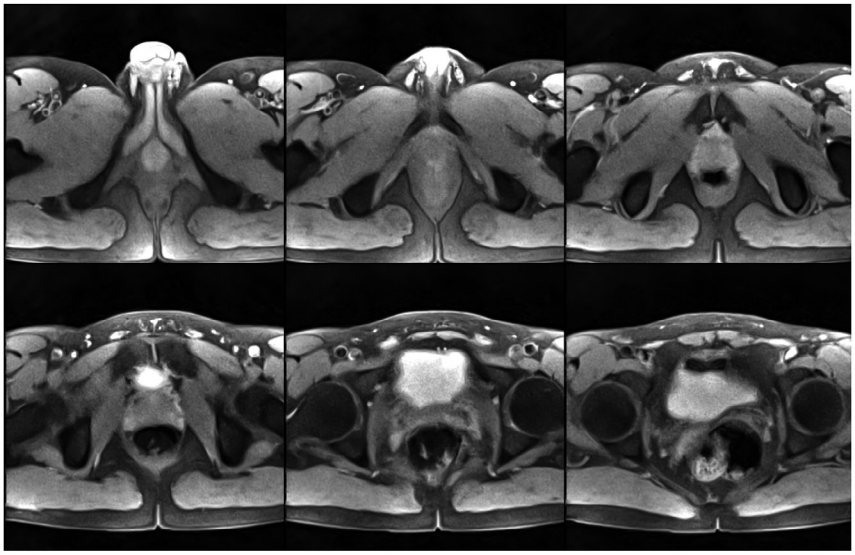

FIGURE 5 Selected fat-suppressed T_2/T_1-weighted images (every 15th) of a 6.0-second real-time MRI acquisition covering the prostate (90-mm volume) of a healthy subject at 66.7 ms and $1.0 \times 1.0 \times 4.0$ mm^3 resolution. For details, see Table 1

The selected T_1-weighted FLASH images were complemented by a fat saturation module comprising a chemical shift selective pulse and gradient spoiler.[10,11] To balance the additional time versus the efficiency of the fat suppression, this 13.4-ms module is repeated only after 3 frames. A related application to the prostate is shown in Figure 5 and Supporting Information Video S5. In this case, a 6.0-second T_2/T_1-weighted scan with fat saturation covers a 90-mm volume (90 sections with 1.0-mm section shift) at 1.0-mm resolution. The experimental parameters closely match the requirements of clinical DCE protocols, but promise better temporal resolution for future perfusion studies.

4 | DISCUSSION

This work presents a novel MRI approach to rapid and motion-insensitive volume coverage. It is based on the principles of cross-sectional real-time MRI, that is, highly undersampled radial gradient-echo sequences in conjunction with regularized nonlinear inverse reconstruction of serial images, which in this case represent successive overlapping sections. Rapid volume coverage may contribute to or complement existing MRI protocols by offering variable contrasts and presaturation options as well as free choices between speed, spatial resolution, and covered volume. The method is highly flexible and may be adjusted according to clinical needs. Typically, as demonstrated here, a 150-mm volume may be scanned at $1.0 \times 1.0 \times 6.0$ mm^3 nominal resolution in around 5.0 seconds.

When compared to a fully sampled radial reference image with FFT reconstruction, but otherwise identical parameters, a limitation of the proposed method is some residual blurring attributable to regularization. This observation compromises the nominal resolution despite the fact that NLINV reconstructions take precautions to ensure convergence. Moreover, the section thickness and section shift should not be too large to avoid the risk of partial volume artifacts in scan direction.

It should also be noted that the motion robustness claimed here holds true for individual cross-sectional images, but not for the scanned volume as a whole. In fact, the insensitivity of a 40- to 50-ms radial image to movements does not mean that different portions of the stack of serial sections cannot be differently affected by a movement. For example, transverse volume coverage of the liver during deep breathing will most likely result in artifact-free cross-sectional images, but precludes a meaningful reformatting of such data into coronal images. Thus, in general, the proposed method for rapid volume coverage is not considered suitable for image reformatting—because it is not a 3D MRI technique. Instead, if information is needed in another spatial orientation, the best approach would be a quick repetition of the scan in that direction.

At this stage, and despite the fact that the NLINV algorithm runs on an integrated GPU computer, a further limitation is the reconstruction speed. For the experimental conditions studied here (Table 1), typical reconstruction times range from 15 to 30 seconds counting from the start of the acquisition until all images are visualized online. This is mainly because of the need for a large number of receive coil elements to properly sample a larger volume. The solution for dynamic real-time MRI of a fixed section is the use of a principal component analysis (PCA) in order to reduce the number of physical coil elements to a few virtual channels. However, for rapid volume coverage, this will require the implementation of a dynamic PCA update for sections moving through the target volume, which involves different sets of receive coil elements. It may further require an update of the automatic body coil reference image, which has recently been integrated into the prep scan period for "seeding" the very first step in the iterative optimization of the very first serial image.[16] This simple technique effectively precludes the eventual occurrence of phase singularities in joint estimations of multicoil MRI data, which correspond to "black holes" in magnitude images.

5 | CONCLUSION

The proposed method allows for rapid and motion-robust scanning of an MRI volume by cross-sectional real-time MRI in a variety of imaging scenarios. Future applications may range from fetal MRI to DCE MRI in different organ systems. However, such ideas remain to be explored in upcoming clinical trials.

CONFLICT OF INTEREST

D.V. and J.F. are co-inventors of a patent and software describing the real-time MRI method used here.

ORCID

Jens Frahm https://orcid.org/0000-0002-8279-884X

REFERENCES

1. Uecker M, Zhang S, Voit D, Karaus A, Merboldt KD, Frahm J. Real-time MRI at a resolution of 20 ms. *NMR Biomed*. 2010;23:986–994.
2. Frahm J, Voit D, Uecker M. Real-time magnetic resonance imaging: radial gradient-echo sequences with nonlinear inverse reconstruction. *Invest Radiol*. 2019 Jul 1. https://doi.org/10.1097/RLI.0000000000000584.
3. Hu HH, Madhuranthakam AJ, Kruger DG, Glockner JF, Riederer SJ. Continuously moving table MRI with SENSE: application in peripheral contrast enhanced MR angiography. *Magn Reson Med*. 2005;54:1025–1031.
4. Fautz HP, Kannengiesser S. Sliding multislice (SMS): a new technique for minimum FOV usage in axial continuously moving-table acquisitions. *Magn Reson Med*. 2006;55:363–370.
5. Börnert P, Aldefeld B. Principles of whole-body continuously-moving-table MRI. *J Magn Reson Imaging*. 2008;28:1–12.
6. Sengupta S, Smith DS, Welch EB. Continuously moving table MRI with golden angle radial sampling. *Magn Reson Med*. 2015;74:1690–1697.
7. Zenge MO, Uecker M, Mattauch G, Frahm J. Continuous table movement MRI in a single breath-hold: Highly undersampled radial acquisitions with nonlinear iterative reconstruction and joint coil estimation. In Proceedings of the 20th Annual Meeting of the ISMRM, Melbourne, Victoria, Australia, 2012. p. 14.
8. Zhang S, Block KT, Frahm J. Magnetic resonance imaging in real time: advances using radial FLASH. *J Magn Reson Imaging*. 2010;31:101–109.
9. Roeloffs VB, Voit D, Frahm J. Spoiling without additional gradients—radial FLASH MRI with randomized radiofrequency phases. *Magn Reson Med*. 2016;75:2094–2099.
10. Haase A, Frahm J, Hänicke W, Matthaei D. 1H NMR chemical shift selective (CHESS) imaging. *Phys Med Biol*. 1985;30:341–344.
11. Frahm J, Haase A, Hänicke W, Matthaei D, Bomsdorf H, Helzel T. Chemical shift selective MR imaging using a whole body magnet. *Radiology*. 1985;156:441–444.
12. Frahm J, Merboldt KD, Hänicke W, Haase A. Flow suppression in rapid FLASH NMR images. *Magn Reson Med*. 1987;4:372–377.
13. Frahm J, Schätz S, Untenberger M, et al. On the temporal fidelity of nonlinear inverse reconstructions for real-time MRI—the motion challenge. *Open Med Imaging J*. 2014;8:1–7.
14. Bakushinsky AB, Kokurin MY. *Iterative Methods for Approximate Solution of Inverse Problems*. Dordrecht, The Netherlands: Springer; 2005.
15. Klosowski J, Frahm J. Image denoising for real-time MRI. *Magn Reson Med*. 2017;77:1340–1352.
16. Voit D, Kalentev O, Frahm J. Body coil reference for inverse reconstructions of multi-coil data—the case for real-time MRI. *Quant Imaging Med Surg*. 2019 Aug 14. https://doi.org/10.21037/qims.2019.08.14.

SUPPORTING INFORMATION

Additional supporting information may be found online in the Supporting Information section.

VIDEO S1 T_2/T_1-weighted movie (20 fps) of a 5.0-second real-time MRI acquisition covering the brain (150 mm volume, 100 sections) of a healthy subject at 50.0 ms and $1.0 \times 1.0 \times 6.0$ mm^3 resolution. fps = frames per second

VIDEO S2 T_1-weighted movie (25 fps) of a 4.0-second real-time MRI acquisition covering the brain (same 150-mm volume and 100 sections as for Supporting Information Video S1) of a healthy subject at 40.0 ms and $1.0 \times 1.0 \times 6.0$ mm^3 resolution. fps = frames per second

VIDEO S3 T_1-weighted movie (25 fps) of a 6.4-second real-time MRI acquisition covering the carotid arteries (128-mm volume, 160 sections) of a healthy subject at 40.0 ms and $0.8 \times 0.8 \times 4.0$ mm^3 resolution. fps = frames per second

VIDEO S4 Fat-suppressed T_1-weighted movie (20 fps) of a 6.0-second real-time MRI acquisition covering the liver (180-mm volume, 120 sections) of a healthy subject at 50.0 ms and $1.2 \times 1.2 \times 6.0$ mm^3 resolution. fps = frames per second

VIDEO S5 Fat-suppressed T_2/T_1-weighted movie (15 fps) of a 6.0-second real-time MRI acquisition covering the prostate (90-mm volume, 90 sections) of a healthy subject at 66.7 ms and $1.0 \times 1.0 \times 4.0$ mm^3 resolution. fps = frames per second

How to cite this article: Voit D, Kalentev O, van Zalk M, Joseph AA, Frahm J. Rapid and motion-robust volume coverage using cross-sectional real-time MRI. *Magn Reson Med*. 2019;00:1–7. https://doi.org/10.1002/mrm.28029